ARTICLE NO. 78-1317

# Missile Guidance for Low-Altitude Air Defense

F. William Nesline*
*Raytheon Company, Bedford, Mass.*

**Practical design considerations for a low-altitude radar-guided air defense missile are presented. Low-altitude target signals return to the receiver mixed with large clutter signals from ground and large multipath signals from smooth sea. The doppler effect and the Brewster angle effect are used to separate true target returns from clutter and multipath contaminations. Sensor design factors, including clutter and multipath rejection, doppler resolution, and sensor stabilization, are discussed in the context of a complete missile guidance and control system. Basic contributors to miss distance are discussed with a quantitative miss distance example showing the role of missile lateral acceleration capability.**

## Nomenclature

$h_M$ = missile height above ground
$h_T$ = target height above ground
$K_S$ = stabilization gain
$m$ = error angle between target and image
$N_0$ = $N_0' V_C / V_M$
$N$ = navigation ratio
$R$ = horizontal missile-to-target range; radome refraction slope
$R_1$ = missile-to-target range
$R_2$ = missile-to-image slant range
$R_{MI}$ = missile-to-image range
$R_{MT}$ = missile-to-target range
$r$ = magnitude of image return relative to magnitude of target return
$T_1$ = seeker tracking time constant
$T_2$ = resultant airframe/autopilot time constant
$T_\alpha$ = missile angle-of-attack to velocity vector angle rate $(\alpha/\dot{\gamma})$
$Y_M$ = missile coordinate
$Y_T$ = target coordinate
$\gamma$ = time to go before intercept
$\dot{\gamma}$ = rate of change of missile velocity vector angle
$\Delta f_D$ = image-target doppler frequency
$\epsilon$ = seeker error angle
$\lambda$ = wavelength
$\lambda_T$ = missile-to-target line-of-sight
$\dot{\lambda}_T$ = rate of change of line-of-sight to the target
$\phi$ = phase angle of resultant relative to target return
$\psi$ = phase angle of $s$
$(\dot{})$ = time derivative

## Introduction

SUCCESSFUL missile guidance for low-altitude air defense poses special problems for the sensing instrument, as well as for the guidance algorithms. The sensor must separate the target return from the clutter return over ground and rough sea. Over smooth water or land, the sensor must separate the target from its image reflected from the surface. In a practical system, the doppler effect is used to separate the ground clutter from the target return, and the Brewster angle effect is used to separate the image return from the target return. Semiactive continuous-wave (CW) guidance is perhaps the most effective implementation of these principles in operational use today to accomplish low-altitude air defense over land and water. This paper describes practical design considerations of such a system, including seeker clutter rejection, feedthrough rejection, doppler resolution, radome refraction slope, and missile acceleration capability. Guidance algorithms and the basic contributors to miss distance are discussed. Quantitative examples of the use of miss distance in system design are given. The fundamental soundness of the principles described in this paper has been proved in many low-altitude air defense systems operational today.

Presented as Paper 78-1317 at the AIAA Guidance and Control Conference, Palo Alto, Calif., Aug. 7-9, 1978; submitted Sept. 12, 1978; revision received Jan. 9, 1979. 

Index categories: LV/M Guidance; Missile Systems; LV/M Dynamics and Control.

*Consulting Scientist and Manager, System Design Laboratory Staff. Member AIAA.

## Principles of Continuous-Wave Semiactive Homing

The basic principles of a continuous-wave (CW) semiactive homing missile system are presented to provide the concepts for evaluation of missile guidance for low-altitude air defense.

A semiactive homing system[1-4] requires a radar to illuminate the target and provide a reference rear signal to the missile. Figure 1 shows these desired signals reeived at the missile, along with the two main undesired signals that cannot be avoided—feedthrough and clutter. Feedthrough is received by the missile directly from the illuminator's main beam, and ground clutter is received by the missile from backscatter of the main beam off the ground.

A representative amplitude-vs-frequency plot of these signals is shown in Fig. 2 for a head-on low-altitude intercept. Because the missile is moving away from the illuminator, the rear reference and feedthrough are frequency shifted down from the transmitted frequency by the doppler frequency $V_M/\lambda$ where $V_M$ is the missile speed and $\lambda$ is the transmitted wavelength. The target signal is shifted up in frequency by $2(V_T+V_M)/\lambda$, where $V_T$ is the target speed. The ground clutter is spread in doppler but peaks near $V_M/\lambda$ above the carrier frequency. When the target signal is detected against the rear reference signal, the feedthrough occurs at zero frequency, the clutter peak is at $2V_M/\lambda$, and the target peaks at $2(V_T+V_M)/\lambda$ or $2V_C/\lambda$, where $V_C$ is the closing speed. Figure 2 also shows the internal system noise generated by the missile receiver. Notice that the signal must be larger than system noise, but both the clutter and the feedthrough can be larger than the target signal. However, because of its doppler shift, the target signal can be separated from these competing signals by a narrow-band filter centered at the target doppler $2V_C/\lambda$. This ability to filter and reject large ground clutter is one reason for the low-altitude effectiveness of CW homing systems.

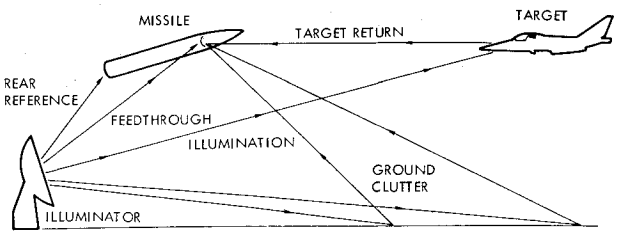


**Fig. 1 Desired and undesired signals.**

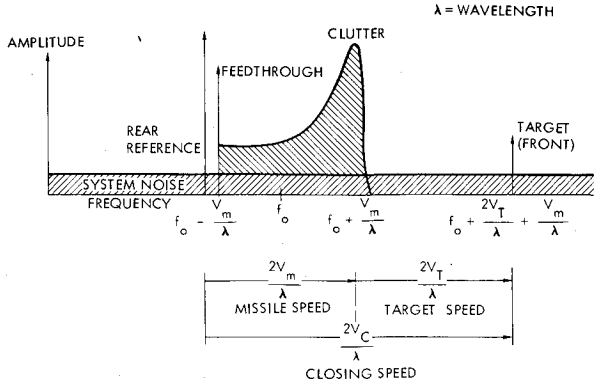


**Fig. 2 Missile signals—amplitude vs frequency.**

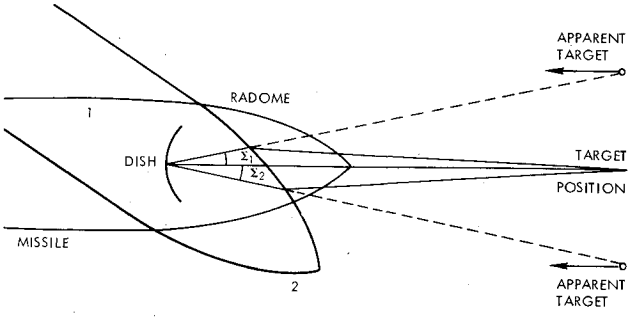


**Fig. 3 Effect of radome refraction slope.**

Since closing speed is a function of the intercept geometry, the doppler filter center frequency must be variable. A closed-loop doppler tracker accomplishes this function. This doppler tracker has two outputs: 1) an output proportional to doppler frequency, which is used to generate closing speed for the proportional navigation guidance law; and 2) the target signal, which is used for angle tracking. The angle tracker's main function is to generate an estimate of the inertial line-of-sight rate. To accomplish this objective, the angle tracker must a) point the seeker antenna at the target to maintain target track, and b) stabilize the seeker against missile pitching motions, which could be interpreted as target motions.

The closing velocity and line-of-sight rate estimates are used to compute acceleration commands that are subtracted from the actual missile acceleration, as measured by an accelerometer. The difference is used to drive control surfaces that generate missile normal force for guidance. This force creates an undesired disturbance because it pitches the missile, thus causing the radome to move with respect to the seeker antenna and the target, resulting in a new equivalent radome refraction angle. The change in angle appears to the seeker exactly like a target line-of-sight rate, as shown graphically in Fig. 3.

The missile and seeker are initially in position 1 with respect to the target, and the missile pitches to position 2. The new position of the radome causes the upper and lower parts of the wavefront to be attenuated differently, which the seeker interprets as a change in angle to the target. The equivalent

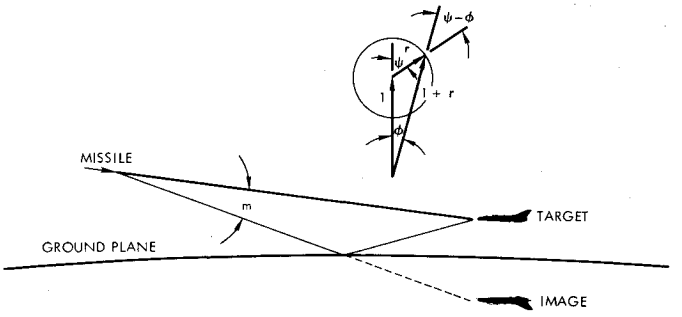


**Fig. 4 Target-image vector diagrams.**

radome refraction can cause a positive $\epsilon_1$ or negative $\epsilon_2$ boresight error shift. Both positive and negative boresight error shifts are important in the design because these shifts increase miss and may actually lead to system instability. To first order, positive shifts lower guidance gain and lengthen the guidance time constant, while negative shifts raise the guidance gain and shorten the guidance time constant to the point where missile instability can occur. The seeker interprets a negative shift as a downward target maneuver and drives the antenna so as to pitch the missile even further down, which is unstable feedback. The guidance design must avoid such an instability.

A good guidance design must also solve the problems of acceleration sensitivity of components, as well as elasticity of the missile structure. These problems will not be considered because they are not unique to semiactive homing systems. However, any CW semiactive homing system must deal with the target doppler shift, reference signal, feedthrough, clutter, seeker tracking, antenna stabilization, and radome refraction slope compensation. The antenna stabilization and the radome refraction effects are important factors in the low-altitude design in that their values and variations influence the achievable effective navigation ratio for homing. When engaging low-altitude targets over highly reflective terrain, the missile's angle tracker must avoid tracking the radar mirror image of the target. Note that the illuminator tracking error is not significant so long as the target is illuminated. In a homing system allowable tracking errors may be large without degrading miss distance, while in a command guidance system such tracking errors lead to large miss distances. The important multipath in the homing system occurs from the interaction of the direct and reflected target return at the missile seeker. However, the missile-to-target geometry produces a steeper grazing angle for the reflected wave than exists for the stationary radar tracking geometry. This steeper grazing angle results in a much smaller reflection coefficient for a vertically polarized wave than for a horizontally polarized wave. In fact, for each frequency and terrain condition, there is a grazing angle (called the Brewster angle) that minimizes the reflection coefficient for vertically polarized waves.[5] Values for the reflection coefficient may be as low as 0.1 or 1.2, even over calm sea. These low values of reflection coefficient mean that if vertical polarization is used, the multipath interference over the flight is minimized. Consequently, the seeker in the final stage of homing resolves the true target from the image and produces small miss even at long range and very low altitudes.

## Guidance Signals during Image Interference

### Target Tracking

Because the semiactive CW seeker guidance signal is completely free of ground clutter, the major contamination of the guidance return signal is from reflection of the target return signal from the surface,[6] as shown in Fig. 4. Over smooth sea or ground, this reflection is mirrorlike, producing an image of the target below the surface. The net signal at the

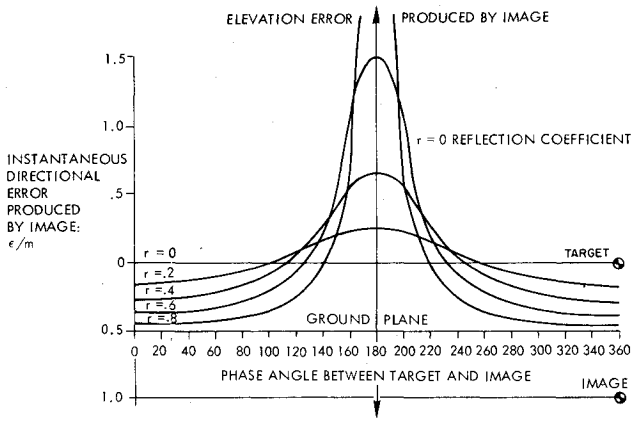


**Fig. 5 Elevation error produced by image.**

seeker is the vector sum of the direct target return and the image return. As the missile and target move toward each other, the phase of the image return rotates with respect to the direct return to prodice resultant amplitude and frequency modulations. For a conical scan seeker the directional error signal is the ratio of the modulation of the composite signal to its amplitude:

$$\epsilon = m \frac{r \cos(\psi - \phi)}{1 \cos\phi + r \cos(\psi - \phi)} \tag{1}$$

where $\epsilon$ is the seeker error angle, $m$ is the error angle between the target and the image, $r$ is the magnitude of the image return relative to the magnitude of the target return, $\psi$ is the phase angle of $s$, and $\phi$ is the phase angle of the resultant relative to the target return.

As the target moves, the boresight error alternates between maximum and minimum values:

$$\epsilon_{max} = m[r/(1-r)] \tag{2}$$

$$\epsilon_{min} = m[r/(1+r)] \tag{3}$$

Figure 5 shows the elevation error produced by an image vs phase angle between the target and the image over the complete cycle of reinforcement and cancellation. Clearly, the average signal is on the target, and as the amplitude of the image return reduces, the angular error fluctuation about the true target signal reduces.

#### Ground Lobes from Target-Image Interference

The effect of target and image enhancement and cancellation is to produce ground lobes. For the geometry shown in Fig. 4, the two path lengths from target to seeker are given by

$$R_1^2 = R^2 + (h_M - h_T)^2 \tag{4}$$

$$R_2^2 = R^2 + (h_M + h_T)^2 \tag{5}$$

where $R_1$ is the missile-to-target slant range, $R_2$ is the missile-to-image slant range, $R$ is the horizontal missile-to-target range, $h_M$ is the missile height above the round, and, $h_T$ is the target height above the ground. The difference in path length is

$$D = R_2 - R_1 = 4h_M h_T/(R_1 + R_2) \tag{6}$$

The lobes of the interference pattern are obtained by letting $D$ equal integral numbers of wavelengths. At long range, compared to the target height, define

$$R_1 + R_2 = 2L \tag{7}$$

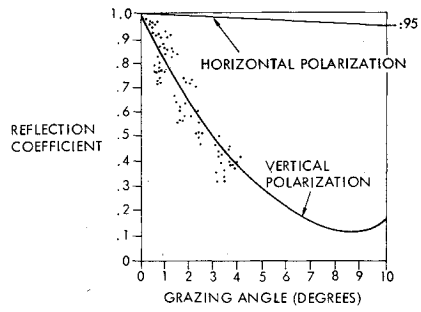


**Fig. 6 Reflection coefficient over smooth sea (λ = 3 cm).**

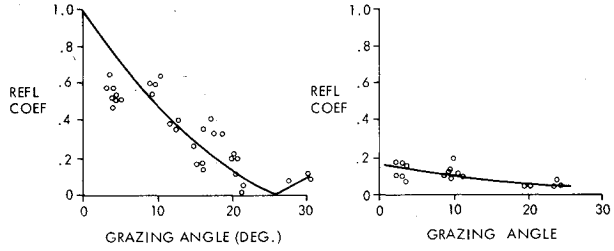


**Fig. 7 Reflection coefficient over land, vertical polarization (λ = 3 cm).**

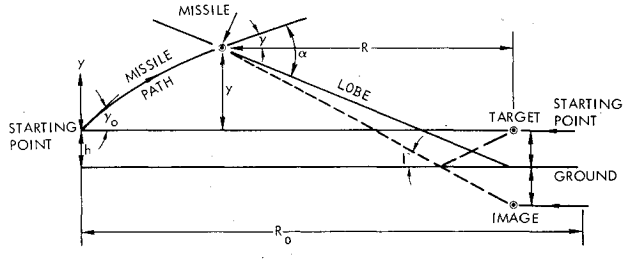


**Fig. 8 Geometry of low-altitude interception problem.**

Then the difference in path length is

$$D = \frac{4h_M h_T}{2L} = \frac{2h_M h_T \cos\theta}{R_0} \tag{8}$$

where $\theta$ is the angle between the lobe and ground, and $R_0$ is the slant range from missile to ground just below the target.

#### Reflection Coefficients

For a radar target located near a reflecting surface, the magnitude of the signal reflected by the surface compared to the magnitude of the direct signal is defined as the reflection coefficient. For horizontal polarization this coefficient is approximately unity for all grazing angles, thereby producing large peaks and deep nulls in the lobing structure. Such a lobing structure leads to erratic tracking of the target. However, if vertical polarization is used, the reflection coefficient drops sharply with increasing grazing angle until a minimum is reached,[7] after which a gradual rise occurs. The value of grazing angle at which this minimum occurs varies from about 8 deg, for 3-cm waves over a smooth sea to 27 deg for dry sandy soil, as shown in Figs. 6 and 7. For missile homing the trajectory can always be shaped to give grazing angles that yield small reflection coefficients—certainly less than 0.5 and more likely in the region less than 0.2.

#### Trajectory Relationships

In a proportional navigation homing missile, the velocity vector turning rate is controlled proportional to the angular

line-of-sight rate to the target:

$$\dot{\gamma} = N\dot{\lambda}_T \tag{9}$$

where $N$ is the navigation ratio, $\dot{\gamma}$ is the rate of change of the missile velocity vector angle, and $\dot{\lambda}_T$ is the rate of change of the line of sight to the target.

From the homing geometry shown in Fig. 8, assuming small angles, a constant missile and target velocity, and a constant altitude target,

$$\lambda_T = \frac{Y_T - Y_M}{R_{MT}} = \frac{Y_T - Y_M}{V_C \tau} \tag{10}$$

where $\lambda_T$ is the missile-to-target line of sight, $Y_T$ is the target coordinate, $Y_M$ is the missile coordinate, $R_{MT}$ is the missile-to-target range, and $\tau$ is the time of flight to go before intercept. Thus

$$\dot{\gamma} = N\frac{\mathrm{d}}{\mathrm{d}t}\left(\frac{Y_T - Y_M}{V_C \tau}\right) \tag{11}$$

or integrating both sides

$$\gamma = (N/V_C\tau)(Y_T - Y_M) + C \tag{12}$$

but

$$\gamma = \dot{Y}_M / V_M \tag{13}$$

Therefore,

$$\dot{Y}_M + \frac{NV_M}{V_C}\frac{Y_M}{\tau} = \frac{NV_M}{V_C}\frac{Y_T}{\tau} + V_M C \tag{14}$$

The solution of this equation for $Y_M$ gives the missile trajectory as a function of time. Note that the trajectory is fixed by the parameter $NV_M/V_C$, defined as $N'$, the effective navigation ratio. Solving, we get

$$\gamma = \frac{\gamma_0 N'}{(N'-1)}\left(\frac{\tau}{\tau_0}\right)^{(N'-1)} - \frac{\gamma_0}{(N'-1)} \tag{15}$$

$$Y_M = \frac{V_M \gamma_0 \tau_0}{N'-1}\left[\left(\frac{\tau}{\tau_0}\right) - \left(\frac{\tau}{\tau_0}\right)^{N'}\right] \tag{16}$$

Where $\tau_0$ is the time of flight at the beginning of the engagement; the missile flies this trajectory through the lobing structure of the target-image interference pattern. The angle between the missile flight path and the particular lobe that the missile is in is given by (see Fig. 8)

$$\alpha = [(Y_M + h)/R] + \gamma(V_M/V_C) \tag{17}$$

The distance between two lobes along this flight path is

$$d = \lambda/2h_T\alpha \tag{18}$$

and the frequency with which lobes are being cut is

$$f = V_C/d \quad \text{lobes/s} \tag{19}$$

Therefore,

$$f = \frac{2h_T\gamma_0 V_M}{\lambda R_0}\left(\frac{\tau}{\tau_0}\right)^{(N'-2)} + \frac{2h_T^2}{\lambda\tau_0 R_0}\left(\frac{\tau_0}{\tau}\right)^2 \tag{20}$$

The minimum frequency is found by differentiating Eq. 20 with respect to $\tau$, setting the result to zero, solving for $\tau_{\min}$,

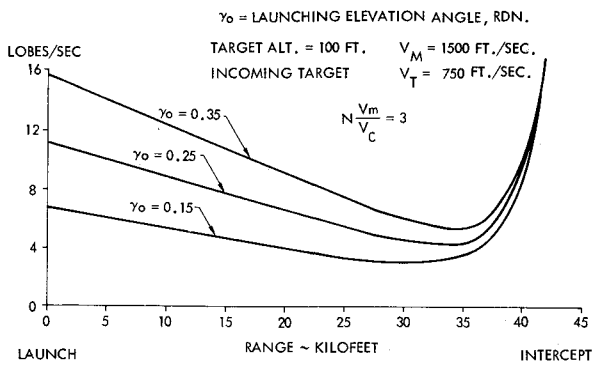


**Fig. 9 Lobe-cutting rate for proportional navigation.**

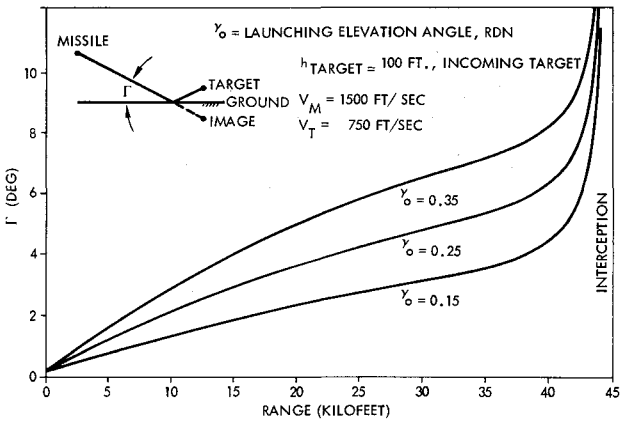


**Fig. 10 Grazing angle during flight.**

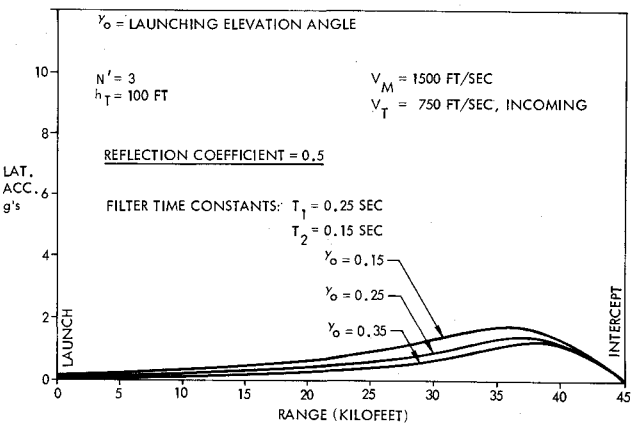


**Fig. 11 Noise produced by lobe cutting.**

and substituting

$$f_{\min} = \left(\frac{h_T}{R_0}\right)^{(2N'-2)/N'} \frac{2N'}{(N'-2)}\frac{V_C}{\lambda}\left[\frac{(N'-2)V_M\gamma_0}{2V_C}\right]^{2/N'} \tag{21}$$

The lobe-cutting rate for a given example is shown in Fig. 9.

The grazing angle during flight determines the reflction coefficient and is

$$\Gamma = \frac{Y_M + 2h_T}{R} \tag{22}$$

$$\Gamma = \frac{V_M\gamma_0}{(N'-1)V_C}\left[1 - \left(\frac{\tau}{\tau_0}\right)^{(N'-1)}\right] + \frac{2h_T}{R_0}\left(\frac{\tau_0}{\tau}\right) \tag{23}$$

Grazing angles for the same application are shown in Fig. 10.

### Guidance Noise from Lobe Cutting

If the homing missile has a guidance bandwidth of 1 to 2 rad/s, and the minimum lobe-cutting rate is 4 to 6 Hz or 25 to 38 rad/s, the missile virtually ignores perturbations in trajectory caused by lobe cutting. The acceleration of the missile caused by lobe cutting for a reflection coefficient of 0.5 is shown in Fig. 11. Note that the maximum acceleration is of the order of 1 to 2 $g$ and that this reduces to zero as the missile appproaches intercept. For a smaller reflection coefficient, the missile acceleration is negligible.

### Doppler Resolution

As the missile dives onto a target over highly reflective terrain, the target return differs from the image return in doppler frequency, as well as in amplitude. If this doppler spread exceeds the doppler tracking speedgate bandwidth, one of the signals will be resolved. After doppler resolution, image interference does not occur. The range at which resolution occurs depends on the doppler bandwidth and the target altitude. A planar formula for differential doppler derived from Fig. 12 is

$$\Delta f_D = \frac{\Delta \dot{S}}{\lambda} \tag{24}$$

$$\Delta \dot{S} = \left[\frac{R_{MT}}{R_{MI}} - 1\right]\dot{R}_{MT} + \frac{2(h_M\dot{h}_T + h_T\dot{h}_M)}{R_{MI}} \tag{25}$$

where

$$R_{MI} = \sqrt{(R_{MT}^2 + 4h_M h_T)}^{1/2} \tag{26}$$

$$\Delta \dot{S} = R_{MI} - R_{MT} \tag{27}$$

For proportional navigation homing the missile velocity vector leads the line-of-sight angle, as shown in Fig. 12. Calculations of target altitude from 100 to 500 ft were made and plotted in Fig. 13 for a 15-deg missile dive angle.

Figure 13 shows that for a 1000-Hz doppler bandwidth, the last 710 ft of homing against a target flying at 100-ft altitude is free of multipath. This is 0.23 s to go, which is not enough time to maneuver. However, if the target altitude is 500 ft, doppler resolution occurs at 3500-ft range. At 1000-ft altitude, resolution occurs at 7000-ft range, which is over 2.3 s to go. Therefore substantial guidance corrections can be made if needed, and the last 2.3 s of flight is completely free of image interference.

### Image Interference Summary

For low-altitude intercepts, interference between the target return signal and its image can occur over highly reflective land or water. Vertical polarization and an appropriate missile dive angle are used to minimize this interference. However, even for relatively high values of reflection coefficient, the missile's flight through the lobbing pattern of the target-image pair produces an angle noise frequency that is high compared to the guidance bandwidth. Therefore, missile acceleration commands caused by multipath interference are small. Finally, the terminal homing dive angle, closing velocity, wavelength, and seeker doppler bandwidth determine a range at which the seeker can resolve the target from the image in doppler frequency. Once this resolution occurs, guidance is completely free of image interference.

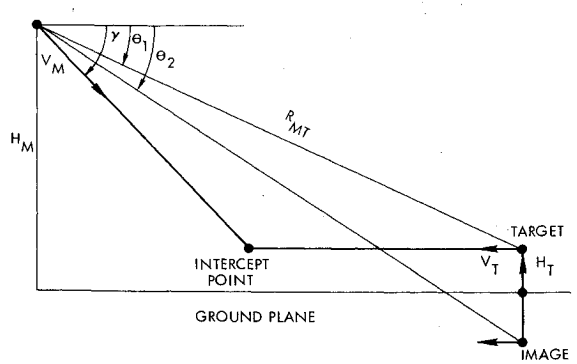


Fig. 12 Doppler resolution geometry.

## Missile Acceleration Effects

### Introduction

The missile acceleration developed from its guidance commands causes body pitch rates that contaminate the line-of-sight rates measured by the seeker. The seeker is stabilized in inertial space to minimize this contamination, but perfect stabilization cannot be achieved. Imperfect stabilization affects homing dynamics by changing both the effective navigation ratio and the missile guidance time constant. However, at low altitude and high velocity, only the change in effective navigation ratio is important because miss is proportional to effective navigation ratio for scintillation, fading, and receiver noise.[3] Radome refraction slope effects modify the degree of imperfect stabilization required to achieve small miss distance at low altitude. In addition to adequate seeker stabilization, it is necessary that the missile be capable of developing adequate acceleration levels to ensure small miss against an accelerating target.

### Guidance Transfer Function

The guidance transfer function with imperfect stabilization and radome refraction slope is derived from the linearized miss distance dynamics depicted in Fig. 14. The miss distance in each case depends on $N'_{eff}$, the effective navigation ratio.[3] The missile trajectory position is computed from its acceleration and subtracted from the target position. This error, when evaluated at the end of the flight, is the miss distance.

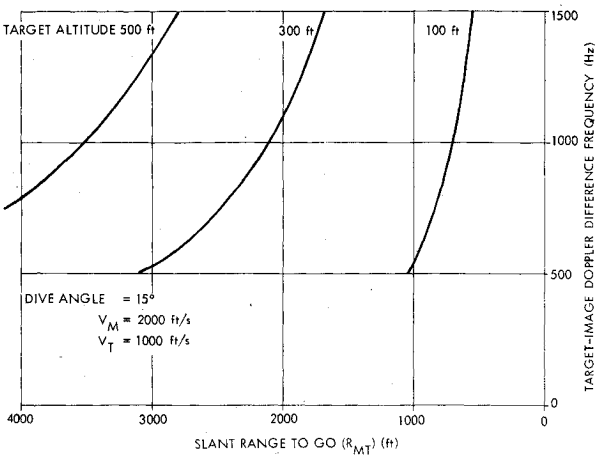


Fig. 13 Target-image doppler frequency.

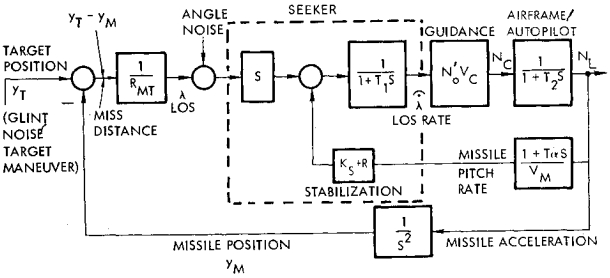


Fig. 14 Linear miss distance dynamics.

Since the seeker measures angles, the position error is divided by range. The seeker dynamics differentiates and smooths this angle to get an estimate of the line-of-sight rate $\dot{\lambda}_T$. Proportional navigation guidance multiplies this estimate by $N'$, the effective navigation ratio, and $V_C$, the closing velocity estimate derived from the doppler tracker. The resulting acceleration command is applied to an acceleration autopilot that moves wind or tail control surfaces so as to develop the commanded acceleration, thus completing the trajectory loop. The rotational loop also derives its input from the missile lateral acceleration. The simplified transfer function to pitch rate is

$$\frac{\dot{\theta}}{N_L} \cong \frac{(1+T_\alpha S)}{V_M} \tag{28}$$

where $T_\alpha$ is the $\alpha/\dot{\gamma}$ time constant. This pitch rate signal drives the seeker's stabilization system, which operates so as to remove missile pitching from the line-of-sight rate estimate. Because stabilization is imperfect, the line-of-sight rate used for guidance will be contaminated by missile pitch motions.

The fundamental signals that contribute to miss distance in Fig. 14 are target maneuver, scintillation noise, and angle noise in the seeker. Target maneuver produces miss only to the extent that missile dynamics are too slow to keep up or that the missile maximum acceleration is inadequate. Scintillation noise is wander of the apparent radar center at the target caused by the complex shape and motion of the target. Angle noise has two components—one is range dependent and the other range independent. Range-dependent noise is receiver noise and is large at long range. Range-independent noise, also called fading noise, is caused by amplitude fluctuations of the target signal that occur at the information frequency in the missile receiver—for example, at the conical scan frequency of a conically scanning missile seeker.[3]

With imperfect stabilization as a simple gain $K_S$ and radome refraction slope as another gain $R$, the transfer function from actual line-of-sight rate, $\dot{\lambda}_T$, to missile acceleration is

$$\frac{n_L}{\dot{\lambda}_T} = \frac{N'_0 V_C}{[1+N_0(K_S+R)]X} \tag{29}$$

where

$$X = \left[1 + \frac{T_1+T_2+N_0T_\alpha(K_S+R)}{1+N_0(K_S+R)}S + \frac{T_1T_2S^2}{(1+N_0(K_S+R)}\right] \tag{29a}$$

where $N_0 = N'_0 V_C/V_M$, $K_S$ is the stabilization gain, $R$ is the radome refraction slope, $T_1$ is the seeker tracking time constant, $T_2$ is the resultant airframe/autopilot time constant, and $T_\alpha$ is the missile angle of attack to velocity vector angle rate $(\alpha/\dot{\gamma})$ time constant. At low altitude and high velocity, the missile-turning-rate time constant $T_\alpha$ is small; so the only significant effects occur in the gain function.

#### Ideal Effective Navigation Ratio

If we solve the ideal proportional navigation equation for missile acceleration due to target acceleration normal to the line of sight, we get

$$\frac{\ddot{y}_M}{\ddot{y}_T} = \frac{N'}{(N'-2)}\left[1-\left(\frac{\tau}{\tau_0}\right)^{N'-2}\right] \qquad (N'>2) \tag{30}$$

or

$$\frac{\ddot{y}_M}{\ddot{y}_T} = -2\,\ell n\left(\frac{\tau}{\tau_0}\right) \qquad (N'=2) \tag{31}$$

Clearly, the effective navigation ratio must be greater than 2 to keep missile acceleration bounded. A typical lower limit on $N'$ is 2.3. At this limit the final missile acceleration level is almost eight times the target acceleration. At $N'=3$, the final acceleration is three times the target's acceleration. The upper limit on $N'$ is determined by the miss due to noise.

#### Imperfect Seeker Stabilization

The effective navigation ratio with zero radome refraction slope is

$$N'_{\text{eff}} = N'_0/(1+N_0K_S) \tag{32}$$

Representative engagement numbers may be $N'_0=3$ and $N_0 = N'_0V_C/V_M = 2.4$. Then if $N'$ is to be kept from dropping below 2.3, $K_S$ must be $\leqq 0.068$.

If engagement factors ($V_C$ and $V_M$) are known ahead of time, $N'_0$ can be adjusted to compensate for this drop in effective navigation ratio. Thus, Fig. 15 shows a plot of

$$K_S = \frac{N'_0 - N'_{\text{eff}}}{N'_{\text{eff}}N'_0(V_C/V_M)} \tag{33}$$

for different values of the parameters $N'_0$ and $N'_{\text{eff}}$ at a given $V_C/V_M$ ratio. A practical stabilization gain might be 0.05, although lower values may be found in state-of-the-art seekers. To achieve an effective navigation ratio of 3 at a stabilization gain of 0.05 requires $N'_0=3.9$. Therefore achievable stabilization gain determines the design value of $N'_0$.

#### Radome Refraction Slope Effects

Radome refraction slope effects modify the stabilization gain setting previously dscribed because $N'_{\text{eff}}$ now changes according to both stabilization gain and its parallel path radome refraction slope.[8] However, unlike $K_S$, the value for $R$ is not a constant but varies over a range of negative to positive values, with the result that the effective navigation ratio cannot be held constant. If $R$ varies $\pm 0.03$, $N'_0=4$, and $K_S=0.055$, then the effective navigation ratio varies as follows:

$$N'_{\text{eff}} = \begin{matrix} 3.48 \text{ at negative } R \\ 2.65 \text{ at positive } R \end{matrix} \tag{34}$$

Therefore we see that practical values of stabilization gain and radome refraction slope interact to determine the attainable effective navigation ratios at low altitude. Achievable miss distance will depend on these navigation ratios.

#### Effect of Limited Missile Acceleration Capability

The missile acceleration capability is especially important at low altitudes where aircraft targets are capable of violent

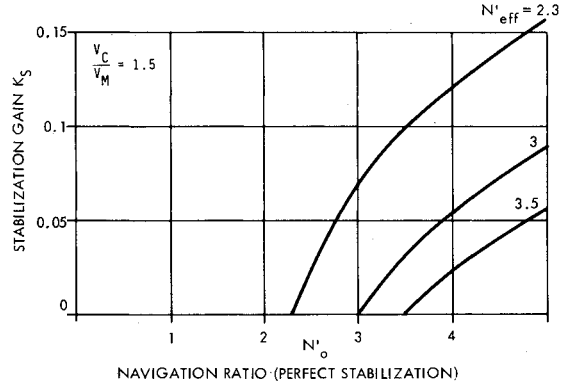


**Fig. 15 Stabilization required to achieve effective navigation ratio.**

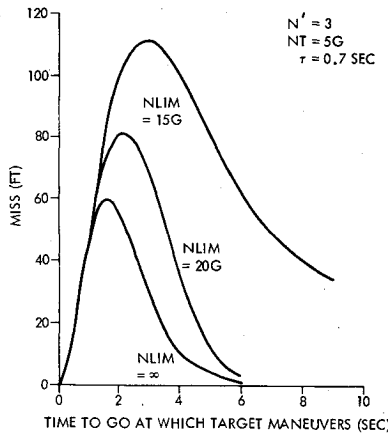


**Fig. 16 Effect of acceleration limit on miss distance.**

maneuvers, particularly if they are trying to evade defensive missiles. Analysis of ideal proportional navigation without time lags given shows that the required missile acceleration is larger than the target acceleration by the factor $N'/(N'-2)$. For $N'=3$, this factor is three, so that a 3-$g$ target maneuver would ideally require a 9-$g$ missile maneuver. Practically, however, the missile must contain time lags as previously discussed. The presence of these time lags increases the acceleration required by the missile. A forward model computer study was performed on the system discussed previously with no radome refraction slope and with perfect stabilization, i.e., $K_S=0$. The missile acceleration limit was included and the results are shown in Fig. 16 for a 5-$g$ target maneuver. If the missile has a long time of flight, it will reduce the miss to zero even with a limited $g$ capability. However a 15-$g$ limit $(3\times N_T)$ yields large miss even at relatively long times of flight. If the missile has an unlimited acceleration capability, the miss reduces to a small number for 5 or 6 s of homing after the maneuver occurs. This performance is approached rather closely by a missile having 20 to 25 $g$. Therefore, we see that the missile should have about five times the maneuvering capability of its targets to obtain the full performance capability of the guidance system.

## Summary and Conclusions

Practical design considerations for a low-altitude radar-guided air defense missile have been presented. The effects of surface clutter have been eliminated by using a semiactive CW seeker. The effects of multipath have been eliminated by using vertical polarization and a lofted trajectory to obtain grazing angles that minimize multipath reflections. The effects of doppler resolution, seeker stabilization, and radome refraction slope on system performance have been discussed. It is shown that, even at low altitudes, seeker stabilization and radome refraction slope interact to influence the effective navigation ratio and hence miss distance caused by noise. The effect of limited missile acceleration on miss distance is discussed, and it is shown that the missile should have about five times the target acceleration capability to attain the full performance capability of the guidance system.

## References

[1] Phillips, T.L., "Anti-Aircraft Missile Guidance," *Electronic Progress,* Raytheon Co., March-April 1958, pp. 1-5.

[2] Long, J.J. and Ivanov, A., "Radar Guidance of Missiles," *Electronic Progress,* Raytheon Co., Fall 1974, pp. 20-28.

[3] Fossier, M.W. and Hall, B.A., "Fundamentals of Homing Guidance," unpublished paper, Raytheon Co., Missile Systems Div., 1961.

[4] Banks, D.S., "Continuous Wave (CW) Radar," *Electronic Progress,* Raytheon Co., Summer 1975, pp. 34-42.

[5] Barton, D.E., *Radar System Analysis,* Prentice-Hall, N.J., 1964, p. 476.

[6] Wisenbaker, T.C., "Image Effects in Missile Seekers," Raytheon Rept. Dec. 22, 1952, presented at Low Altitude Target Problem Symposium at Redstone Arsenal, Jan. 6-8, 1953.

[7] Sherwood, E.M. and Ginzton, E.L., "Reflection Coefficients of Irregular Terrain at 10 cm," *Proceedings of IRE,* No. 7, July 1955, p. 877.

[8] Peterson, E.L., *Statistical Analysis and Optimization of Systems,* Wiley, New York, 1961, pp. 61-62.